EFFECT OF STIMULATED AND THERMAL DESORPTION IN DARHT-2

T. P. Hughes*, MRC, Albuquerque, NM, USA, H. Davis† LANL, Los Alamos, NM, USA

Abstract

The DARHT-2 accelerator generates a 2 kA, 18 MeV, 2 μsec flat-top electron beam. The beam risetime is about 700 ns, and a "beam cleanup zone" (BCUZ) has been designed to scrape off these mismatched electrons. Experiments on DARHT-1 (which has a 60 ns flat-top) have provided excellent quantitative data on stimulated and thermal desorption of neutral monolayers on various metal surfaces by multi-MeV electrons. We have used these data in the particle-in-cell code LSP to model the production of ions from the walls of the DARHT-2 BCUZ. The effect of these ions on the transport of the main beam pulse is discussed.

INTRODUCTION

The DARHT-2 linear induction accelerator [1] is designed to produce a 2 kA, 18 MV, 2 μs flat-top electron beam. The injector is driven directly by a Marx bank, and has a long voltage risetime: 1–99% in 700 ns. As a result, there is a considerable amount of beam charge which is mismatched to the solenoid transport channel. The design of a "beam cleanup zone" (BCUZ) to filter out this charge was previously described [2]. In this paper, we present a computational estimate of the ion charge produced by beam electrons striking the walls of the BCUZ. The computational model uses data from experiments carried out on DARHT-1 [3], a companion accelerator with a 60 ns beam pulse [1].

COMPUTATIONAL MODEL

Beam Generation

The DARHT-2 injector geometry is shown in Fig. 1. A 10 m sections of beam pipe is modeled in $2\frac{1}{2}$-D using the electromagnetic particle-in-cell (PIC) simulation code LSP[4]. The transmission line attached to the radial boundary at T_{AK} in Fig. 1 produces the voltage pulse shown in Fig. 2 [5]. The cathode is treated as a zero-work-function, space-charge-limited emitter. Emitted electrons are given a transverse temperature corresponding to the surface temperature ($\approx 1000^\circ$ C). The beam electrons pass through the accelerating gaps and solenoidal fields of the first eight accelerating cells. As in the physical accelerator, each gap in the simulation is powered by a separate transmission line attached at the boundary (T_1–T_8 in Fig. 1). The accelerating voltage, also shown in Fig. 2, is based on the experimentally-measured voltage trace [5]. The magnetic tune, shown in Fig. 3 was chosen to avoid any beam-loss

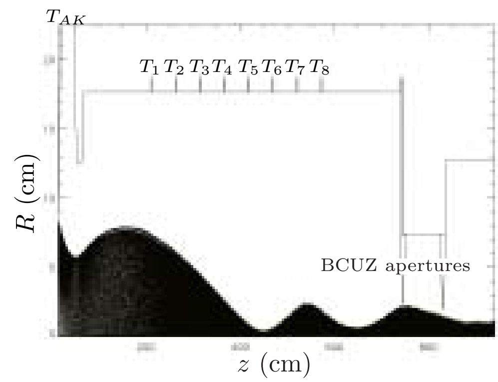

Figure 1: Geometry of desorption calculation, showing injector, 8 accelerating gaps, and BCUZ. The beam is shown at the flat-top energy and current.

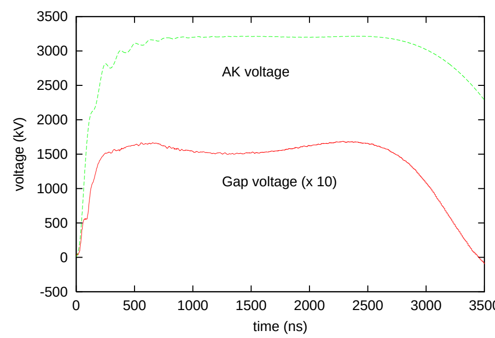

Figure 2: Voltage pulse applied to AK gap (green) and to accelelerating gaps (red). The latter has been multiplied by 10 for scaling purposes.

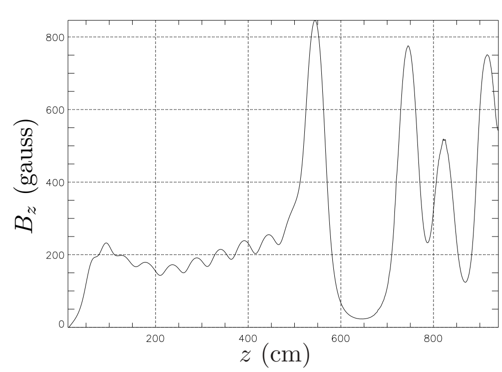

Figure 3: Axial magnetic field tune used in Fig. 1.

* tph@mrcabq.com
† davis@lanl.gov

in the accelerating cells, and to scrape off the beam-head in the BCUZ[2]. In the simulation, we see no beam loss until the start of the BCUZ, about 6 meters from the cathode.

Ion Generation Model

When energetic electrons strike a solid surface, they can generate neutral molecules and ions. There are two mechanisms for generating neutrals: stimulated desorption (ESD) and thermal desorption. Ions can be generated directly by ESD and by a two-step process of neutral desorption followed by ionization. In LSP, these processes are modeled by the following equations:

$$\frac{dN_d^n}{dt} = \frac{j_e}{e}\sigma_d^n N_a + N_a \nu \exp\left(-\frac{Q_b}{T}\right) \quad (1)$$

$$\frac{dN_d^+}{dt} = \frac{j_e}{e}\sigma_d^+ N_a \quad (2)$$

$$\frac{d(N_d^n + N_d^+)}{dt} = -\frac{dN_a}{dt} \quad (3)$$

$$\frac{dN_i}{dt} = \frac{j_e}{e}\sigma_i N_d \quad (4)$$

where N_d^n is the area density of desorbed neutral particles, N_a is the area density of adsorbed particles, N_d^+ is the area density of desorbed ions, N_i is the area density of ions due to gas-phase ionization, σ_d^n, σ_d^+ and σ_i are the cross-sections for stimulated desorption of neutral species, stimulated desorption of ionized species, and gas-phase ionization of the neutral species, respectively, j_e is the electron current density striking the wall, ν is a thermal-desorption rate-constant (typically 10^{13} s^{-1}), Q_b is the binding energy of the adsorbed material in eV, and T is the surface temperature in eV.

In the calculation, we initialize the surfaces with one monolayer (10^{15} cm^{-2}) of neutral water. In the DARHT-1 experiments [3], the stimulated neutral desorption yield, $N_a\sigma_d^n$, was measured to be in the range 0.1–0.2, and the adsorbed inventory was estimated to be about 1 monolayer, mainly consisting of water. Thermal desorption became significant when the surface temperature increased by 300–400° C. Roughly, a desorption rate of one monolayer/ns occurs when the surface temperature reaches $Q_b/9$ eV, which corresponds to about 630 K ($\approx 330°$ C above room temperature) for $Q_b = 0.5$ eV, a typical value for water vapor [6]. At room temperature (300 K) the desorption rate is a factor of 2×10^4 smaller.

Neutrals produced by either stimulated or thermal desorption can be ionized by subsequent beam electrons. We use the gas-phase cross-section for water molecule ionization by relativistic electrons: $\sigma_i = 0.9 \times 10^{-18}$ cm^2 [7]. Water is known to “crack” under electron impact, producing significant fractions of OH^+ and H^+, in addition to H_2O^+ [8]. We have not included these species in the calculation.

Direct stimulated production of ions was not measured in the DARHT-1 experiments. Typically, the cross-section for producing ions is much less than that for neutrals [9].

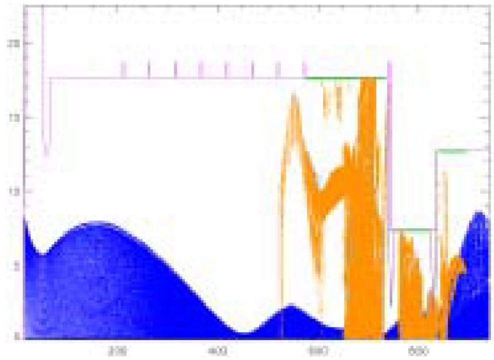

Figure 4: Beam (blue) and H_2O^+ (orange) distributions at $t = 1000$ ns; cf. Fig. 1.

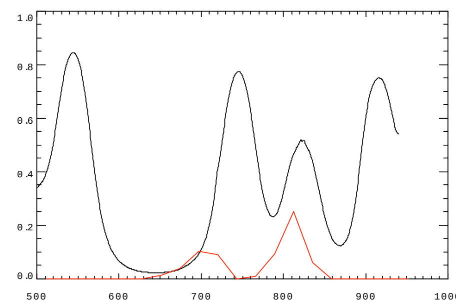

Figure 5: Ratio of ion (H_2O^+) charge to beam charge vs. z at $t = 1000$ ns, within a radius of 1.5 cm (red line). The axial solenoidal magnetic field in kilogauss is overplotted (black). Horizontal scale is in cm.

We have used a value $\sigma_d^+ = 0.01\sigma_d^n = 2 \times 10^{-18}$ cm^2 in the calculation.

EFFECT ON THE ELECTRON BEAM

Ions resulting from stimulated desorption or from ionization of desorbed neutrals can affect the tune and stability of the electron beam. A snapshot of the particle distribution at $t = 1000$ ns is shown in Fig. 4. By this time, about 1000 μC of beam electron charge has struck the wall, yielding about 2 μC of stimulated ion charge. Taking the line-ratio of stimulated ion charge to beam charge within a radius of 1.5 cm from the axis, we get the results shown by the red line in Fig. 5. The dominant contribution to the ion line-density is from stimulated ions. The number of ions generated from desorbed neutrals is much less: the surface temperature rises by at most 50° C, as shown in Fig.6. From Fig. 7 is clear that the ions have a large effect on the beam exiting the BCUZ. We can convert the line-charge ratio f to an equivalent magnetic field through the relation

$$B_{eff} \approx 3.4\sqrt{2\nu\gamma f}/r_b \qquad \text{kG} \qquad (5)$$

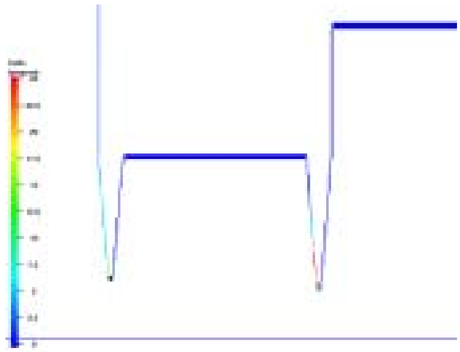

Figure 6: Surface temperature rise (K), in the BCUZ region at the end of the beam risetime.

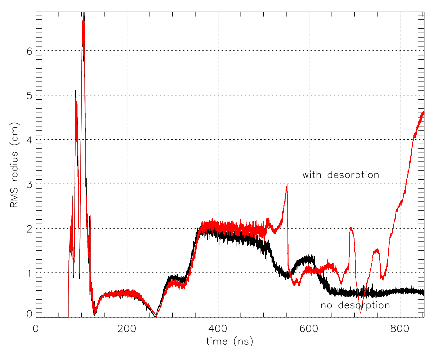

Figure 7: RMS beam radius at $z = 938$ cm with (red line) and without (black line) the effect of desorbed ions.

where ν is Budker's parameter for the beam current and r_b is the beam radius in cm. Thus, the first peak in f in Fig. 5 is roughly equivalent to a 1 kG field extending over 30-40 cm, comparable to the actual focusing solenoids in Fig. 5.

CONCLUSIONS

Beam deposition on the walls of the DARHT-2 beam cleanup zone generates ions through direct stimulated desorption and through neutral desorption followed by impact ionization. For lack of data, the stimulated ion yield used in the calculation is a free parameter. For a sample value equal to 1% of the measured neutral yield, there is a large disruption of the beam. Experimental data on the stimulated ion yield is needed to make a prediction for how large the effect will be in the actual machine.

ACKNOWLEDGMENTS

This work was supported by Los Alamos National Laboratory. The simulations were carried out on the Qsc parallel computer under an Institutional Computing grant from LANL.

REFERENCES

[1] M.J. Burns, B.E. Carlsten, H.A. Davis, C.A. Ekdahl, C.M. Fortgang, B.T. McCuistian, F.E. Merrill, K.E. Nielsen, C.A. Wilkenson, K.P. Chow, W.M. Fawley, H.L. Rutkowski, W.L. Waldron, S.S. Yu, G.J. Caporaso, Y.-J. Chen, E.G. Cook, S. Sampayan, J.A. Watson, G.A. Westenskow, and T.P. Hughes. Status of the DARHT phase 2 long-pulse accelerator. In *Proceedings of the 2001 Particle Accelerator Conference*, number 01CH37268C (http://accelConferenceweb.cern.ch/AccelConf/p01/-PAPERS/WOAA008.PDF).

[2] T.P. Hughes, D.P. Prono, W.M. Tuzel, and J.R. Vananne. Design of beam cleanup zone for DARHT-2. In *Proceedings of the 2001 Particle Accelerator Conference*, number 01CH37268C, (http://accelConferenceweb.cern.ch/AccelConf/p01/-PAPERS/RPPH038.PDF).

[3] H. Davis, D. Moir, and R. Olson. Measurements of thermally desorbed ions from beam-target interactions. In *Proceedings of the 2003 Particle Accelerator Conference*, 1993. Paper ROPB003.

[4] LSP is a software product of Mission Research Corporation (http://www.mrcabq.com).

[5] M. Kang and K. Nielsen, 2003. Private communication.

[6] M.E. Cuneo. The effect of electrode contamination, cleaning and conditioning on high-energy pulsed-power device performance. *IEEE Trans. Dielectr. Electr. Insul.*, 6:469, 1999.

[7] T. C. Genoni and T. P. Hughes. Ion-hose instability in a long-pulse linear induction accelerator. *Phys. Rev. ST Accel. Beams*, 6, 030401, 2003.

[8] M. V. V. S. Rao, I. Iga, and S.K. Srivastava. Ionization cross-sections for the production of positive ions from H2O by electron impact. *J. Geophys. Res.*, 100:26421, 1995.

[9] T. E. Madey and J. T. Yates, Jr. Electron-stimulated desorption as a tool for studies of chemisorption: A Review. *J. Vac. Sci. Technol.*, 8(4):525, 1971.